Carrera Unified Formulation (CUF) for the analysis of disbonds in Single Lap Joints (SLJ)

Carrera unified formulation (CUF) for the analysis of disbonds in single lap joints (SLJ)

Francesco Nicassio, Maria Cinefra, Gennaro Scarselli, Matteo Filippi, Alfonso Pagani, et al.

Francesco Nicassio, Maria Cinefra, Gennaro Scarselli, Matteo Filippi, Alfonso Pagani, Erasmo Carrera, "Carrera unified formulation (CUF) for the analysis of disbonds in single lap joints (SLJ)," Proc. SPIE 12047, Nondestructive Characterization and Monitoring of Advanced Materials, Aerospace, Civil Infrastructure, and Transportation XVI, 1204702 (18 April 2022); doi: 10.1117/12.2616542

SPIE.

Event: SPIE Smart Structures + Nondestructive Evaluation, 2022, Long Beach, California, United States

Carrera Unified Formulation (CUF) for the analysis of disbonds in Single Lap Joints (SLJ)

Francesco Nicassio[a], Maria Cinefra[b], Gennaro Scarselli[a], Matteo Filippi[c], Alfonso Pagani[c], and Erasmo Carrera[c]

[a]Department of Innovation Engineering, University of Salento, Lecce, Italy
[b]Department of Mechanics, Mathematics & Management, Politecnico of Bari, Bari, Italy
[c]Department of Mechanical and Aerospace Engineering, Politecnico of Torino, Torino, Italy

ABSTRACT

The aim of this work is the study of the adhesion integrity of metallic Single Lap Joints (SLJs) through the assessment of the MUL^2 CODE, software developed by the MUL^2 Research Group - Department of Mechanical and Aerospace Engineering of Politecnico di Torino. The MUL^2 CODE is implemented through the Carrera Unified Formulation (CUF) for 2D structures based on Hierarchical Legendre Expansion (HLE) polynomials. An efficient method for the Structural Health Monitoring (SHM) of bonded joints is simulated and verified by CUF approach, in order to reduce the computational cost of analyses: by using transient excitations (toneburst signals), the structural health of damaged SLJ can be numerically evaluated. The interaction mechanism between the waves traveling through the investigated specimens is numerically modeled with a simple Finite Elements (FE) model and it is solved via MUL^2 CODE and commercial software Ansys Workbench, respectively. Experimental campaigns data are compared with CUF and Ansys results demonstrating the consistence of the MUL^2 formulation that is computationally simpler, but very efficient for the joint analysis. The presented and discussed CUF application is able to quantify with a high accuracy the debonding extension in the damaged SLJ, simply tuning the excitation frequency of the SHM technique.

Keywords: Carrera Unified Formulation, Structural Health Monitoring, Single Lap Joints, Local Defect Resonance

1. INTRODUCTION

The simulation of ultrasonic guided waves in thin-walled structures is a challenging task for several reasons. First, these waves can travel long distances with low levels of attenuation, therefore the domain of analysis become usually very large. In addition, the short wavelengths and periods involved in the mechanical problem call for very fine discretizations both in space and in time. Many analytical methods were developed in the last decades focusing on the obtention of the dispersion relations and the wavefront characteristics. Among these, the transfer matrix method[1] and the global matrix method[2] are the most popular in the field. Semi-Analytical Finite Element (SAFE) methods[3–5] were also generated by exploiting the versatility of the Finite Element Method (FEM) in some directions where the discontinuities in the material and geometry could not be described analytically. Three dimensional approaches such as Local Interaction Simulation Approach (LISA),[6,7] based on explicit finite differences, and the Mass-Spring Lattice Method (MSLM)[8] were also introduced. Minimal models based on ray-tracing techniques and stored data of the dispersion curves can be found in the literature as well.[9] The aforementioned models provide fast solutions for certain study cases, but their application to complex 3D geometries involving scattering of the waves caused by arbitrary defects is not a straightforward task, therefore numerical methods are often preferred in these cases.

Most studies on the interaction of ultrasonic waves with discontinuities and defects were carried out using FEM or similar techniques.[10–13] However, when dealing with these problems, weak-form solutions such the FEM must always respect certain refinement constrains to compute acceptable results. Specifically, the element

Further author information: (Send correspondence to F.N.)
F.N.: E-mail: francesco.nicassio@unisalento.it. Website: https://sites.google.com/unisalento.it/asselab

Nondestructive Characterization and Monitoring of Advanced Materials, Aerospace, Civil Infrastructure, and Transportation XVI, edited by H. Felix Wu, Andrew L. Gyekenyesi, Peter J. Shull, Tzuyang Yu, Proc. of SPIE Vol. 12047, 1204702 · © 2022 SPIE · 0277-786X · doi: 10.1117/12.2616542

length should be smaller than the minimum wavelength, which for ultrasonic waves are typically very short. This limitation, together with the small time steps required for transient analyses, and the large spatial domains which are required for damage detection simulations, makes the use of standard FEM extremely expensive from the computational point of view.

In order to increase the efficiency of the numerical simulations in wave propagation problems, a commonly adopted technique is to make use of sets of higher-order shape functions to interpolate the displacement variables. Inspired by this approach, many methods have been recently proposed for the computation of the time signals, such as the Spectral Element Method (SEM),[14,15] the IsoGeometric Analysis (IGA),[16,17] the spectral cellmethod,[18] the enriched finite element method[19] and the p-version of FEM.[20] In the latter work, a comparison between some of these higher-order elements was presented and it is shown that the superiority of higher-order approaches with respect to commercial low-order FEM in terms of convergence rates. Since ultrasonic wave-based systems are used in thin-walled structures, the geometry of the domain requires the use of dimensionally reduced theories of structure, i.e. plates. These models permit to overcome the aspect ratio constrains of 3D FEM by adopting mathematical assumptions on the transverse directions. Some examples of the use of plate elements based on 2D SEM for SHM simulations can be found in the literature.[15,21] In particular, due to their lower computational costs, 2D elements allow for the study of the propagation of ultrasonic waves in real aerospace structures.[22,23] However, one must be aware that the simple approximation in the transverse direction of classical plate theories presents some drawbacks: (1) the symmetric modes may be neglected or poorly approximated, (2) the quality of the numerical simulation (computed phase and group speeds) is significantly reduced, as it is proven in,[24] (3) higher-order modes cannot be studied with enough accuracy.

The present work proposes the use of advanced structural theories in the framework of Carrera Unified Formulation (CUF)[25] to overcome most of the issues of classical structural theories for the simulation of ultrasonic waves. In essence, making use of CUF as a generator of structural models, the displacement assumptions in the transverse plane are enriched using different sets of higher-order polynomials.[26] In this manner, the complex mode shapes of the ultrasonic waves can accurately be captured with no need of 3D discretizations, thus reducing the computational cost of the analysis. In particular, the main goal of the present research is to validate CUF models in simulating ultrasonic waves propagating in two bonded plate for the detection and sizing of a debonding region. Using CUF and recognizing the importance of the correct through-thickness distributions of displacements and stresses, a delamination model was implemented in recent works[27,28] for the free-vibration analysis of delaminated composite plates and shells. In light of the conclusions drawn in those works, layer-wise models are directly chosen for the present analyses because of the possibility to consider the layers separately and its resulting high accuracy. The final aim, to be pursued in a companion work, will be to apply the same models to the detection of delaminations in multilayered composite plates, where the CUF turns out to be particularly convenient in terms of computational efficiency.

2. MATERIALS, EXPERIMENTAL & NUMERICAL METHOD

2.1 Specimens & Experimental Setup

Testing samples were made of two plates with an overlap zone equal to 30 mm. The plate material was the aluminum since its mechanical properties are well known and easy to be simulated, while the adhesive layer was an acrylic film with elastic modulus equal to 3.69 GPa, density of 1300 kg/m^3 and Poisson ratio equal to 0.3. The adhesive zone was artificially damaged by inserting a Teflon patch between the layer and the upper aluminium plate: when the shear stresses exceed the maximum allowed value at the edges of the adhesion area, the adhesive fails as in the experimental samples. Furthermore, in order to avoid that the boundary conditions strongly affect the ultrasonic waves propagation through the specimen, two sponges at the two ends simply supported the SLJ. Different disbonds lengths (Deb) were investigated and each experimental campaign was repeated five times in order to verify its repeatability. The artificial debonding area and the experimental setup are shown in Figure 1.

The "workflow" of the experimental campaign is the following.

1. The signal generator TG5012A (Aim & Thurlby Thandar Instrument) (top-right corner in Figure 1) produces the toneburst signals (according to the technique presented in[29])...

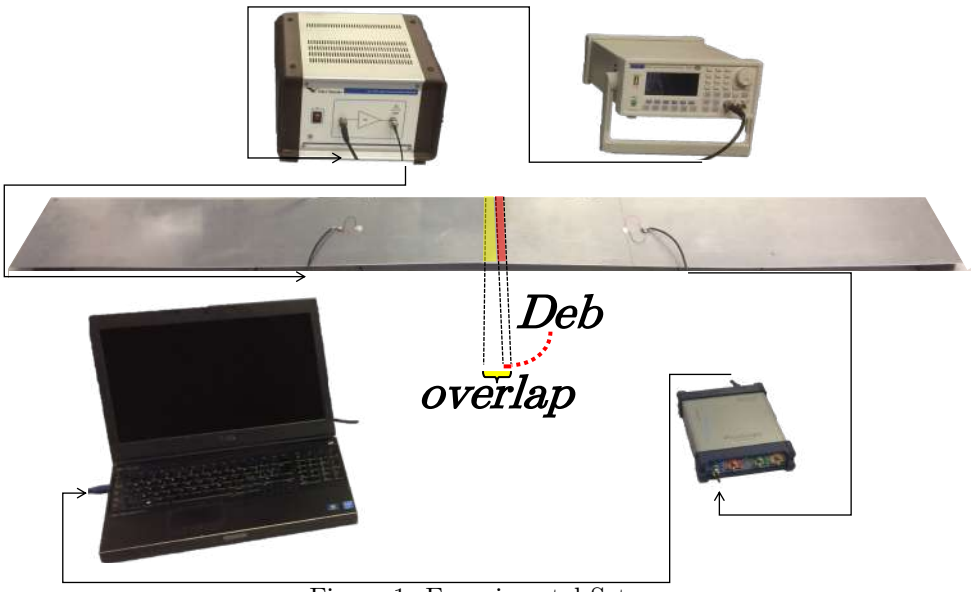

Figure 1: Experimental Setup.

2. ... to the power-amplifier Falco System WMA-300 (top-left corner in Figure 1) that multiplied by 50 the input voltage.
3. The left piezo-sensor is excited with high purity toneburst waves, low harmonic distortion, low phase noise;
4. then the right sensor receives the transmitted waves and sends them...
5. ... to the oscilloscope Serie 3000 PicoScope (bottom-right corner in Figure 1).
6. Eventually, the real-time acquisition of the propagating waveforms is performed with a portable PC (bottom-left corner in Figure 1) and subsequently post-processed, using PicoScope 6 software and MATLAB codes in order to detect the several investigated damage lengths.

The analytical approach. presented by Nicassio et al. in[29] and used for describing the wave propagation in the specimen is briefly shown. The Lamb waves originated by the exciting sensor travels through the aluminium plate and two different joint regions (overlap and Deb areas in Figure 1) with different speeds: (i) c_{ov} in the overlap region, where the waves travels through three layers (top plate, adhesive ply and bottom plate), (ii) c_{al} in the Deb region, where the wave travels through the top plate, reaches the edge and is reflected. At the line between overlap and Deb zone there is interference between the two waves. So, a toneburst (with N number of peaks) can be sent though the SLJ and its frequency can be tuned until a destructive interference appear. Through the Equation 1 this frequency f_{att} is directly related to the defect extension Deb.

$$f_{att} = \frac{N\left(c_{ov} - c_{al}\right) + c_{al}}{4Deb} \tag{1}$$

2.2 Layer-Wise 2D models based on Carrera Unified Formulation

As explained in many previous works related to the Carrera Unified Formulation, classical theories have several limitations. The main point is that, in order to predict higher order effects and overcome the physical inconsistencies, the kinematics should be theoretically enriched with an infinite number of terms (see Washizu[30]). This is obviously not possible from a practical point of view and the theories of structure are generally formulated by truncating the expansion of the primary mechanical variables (along the smallest dimensions of the structure domain) to a given order. Nevertheless, the more the terms in the kinematics, the more the complexity of the formulation and resolution of the problem is. The Carrera Unified Formulation (see[31,32]) solves this issues by

describing the kinematic field in a unified manner that will be then exploited to derive the governing equations in a compact way.

Let us consider a generic multilayered plate structure whose mid-plane lays in the xy-plane, with respect to a Cartesian coordinate system. The displacement field of two-dimensional models in CUF framework is described as a generic expansion of the generalized displacements (in the case of displacement-based theories) by arbitrary functions of the thickness coordinate z (see[33]):

$$\mathbf{u}(x,y,z) = F_\tau(z)\mathbf{u}_\tau(x,y) \quad \tau = 1,2,...,M \tag{2}$$

where $u = \{u_x, u_y, u_z\}$ is the vector of 3D displacements and $u_\tau = \{u_{x\tau}, u_{y\tau}, u_{z\tau}\}$ is the vector of general displacements, M is the number of terms in the expansion, τ denotes summation and the functions $F_\tau(z)$ define the 2D model to be used. In fact, depending on the choice of $F_\tau(z)$ functions, different classes of plate theories can be implemented.
In this paper, only Lagrange expansions are considered, but other types of expansions based on the use of Taylor or Legendre polynomials can be conveniently employed as discussed in many previous works by Carrera et al.[32,34,35]

Layer-wise plate theories based on Lagrange expansion (see[32,36,37]) are formulated by adopting 1D Lagrange polynomials as F_τ thickness functions (up to the desired order p) and expanding the variables independently in each layer k:

$$\begin{array}{l} u_x^k = F_1(\zeta)\, u_{x_1}^k + F_2(\zeta)\, u_{x_2}^k + F_i(\zeta)\, u_{x_i}^k \\ u_y^k = F_1(\zeta)\, u_{y_1}^k + F_2(\zeta)\, u_{y_2}^k + F_i(\zeta)\, u_{y_i}^k \\ u_z^k = F_1(\zeta)\, u_{z_1}^k + F_2(\zeta)\, u_{z_2}^k + F_i(\zeta)\, u_{z_i}^k \end{array} \tag{3}$$

where i denotes a summation and ranges from 1 to $p+1$.
Lagrange polynomials have been extensively employed in the formulation of variable kinematics plate and shell theories in a unified framework by Kulikov and his co-workers. The readers are referred to the original papers for more details about 2D models based on Lagrange-type expansions, see for example.[38,39]

2.2.1 Finite element formulation

The main advantage of CUF is that it allows to write the governing equations and the related finite element arrays in a compact and unified manner, which is formally an invariant with respect to the F_τ functions. In the sections below, the mathematical derivation of the fundamental nuclei of the stiffness matrix and mass matrix in the case of CUF 2D models is provided in detail.

2.2.2 Geometrical relations and constitutive equations

According to classical elasticity theory, stress and strain tensors of each layer can be organized in six-term vectors with no lack of generality. They read, respectively:

$$\begin{array}{l} \boldsymbol{\sigma}^{kT} = \left\{ \begin{array}{cccccc} \sigma_{yy}^k & \sigma_{xx}^k & \sigma_{zz}^k & \sigma_{xz}^k & \sigma_{yz}^k & \sigma_{xy}^k \end{array} \right\} \\ \boldsymbol{\varepsilon}^{kT} = \left\{ \begin{array}{cccccc} \varepsilon_{yy}^k & \varepsilon_{xx}^k & \varepsilon_{zz}^k & \varepsilon_{xz}^k & \varepsilon_{yz}^k & \varepsilon_{xy}^k \end{array} \right\} \end{array} \tag{4}$$

Regarding to this expression, the geometrical relations between strains and displacements with the compact vectorial notation can be defined as:

$$\boldsymbol{\varepsilon}^k = \mathbf{D}\,\mathbf{u}^k \tag{5}$$

where, in the case of small deformations and angles of rotations, $\mathbf{D}$ is the following linear differential operator:

$$\mathbf{D} = \begin{bmatrix} 0 & \frac{\partial}{\partial y} & 0 \\ \frac{\partial}{\partial x} & 0 & 0 \\ 0 & 0 & \frac{\partial}{\partial z} \\ \frac{\partial}{\partial z} & 0 & \frac{\partial}{\partial x} \\ 0 & \frac{\partial}{\partial z} & \frac{\partial}{\partial y} \\ \frac{\partial}{\partial y} & \frac{\partial}{\partial x} & 0 \end{bmatrix} \tag{6}$$

On the other hand, for multilayered composite materials the relation between stresses and strains is obtained through the generalized Hooke's law:

$$\boldsymbol{\sigma}^k = \mathbf{C}^k \boldsymbol{\varepsilon}^k \tag{7}$$

where $\mathbf{C}^k$ is the matrix of elasticity coefficients of the arbitrarily oriented orthotropic layer with respect to the global reference system (x, y)

$$\mathbf{C}^k = \begin{bmatrix} C_{22}^k & C_{12}^k & C_{23}^k & 0 & 0 & C_{16}^k \\ C_{12}^k & C_{11}^k & C_{12}^k & 0 & 0 & C_{26}^k \\ C_{23}^k & C_{12}^k & C_{33}^k & 0 & 0 & C_{36}^k \\ 0 & 0 & 0 & C_{55}^k & C_{54}^k & 0 \\ 0 & 0 & 0 & C_{45}^k & C_{44}^k & 0 \\ C_{16}^k & C_{26}^k & C_{36}^k & 0 & 0 & C_{66}^k \end{bmatrix} \tag{8}$$

The coefficients C_{ij}^k depend on the Young's moduli E_1, E_2, E_3, the shear moduli G_{12}, G_{13}, G_{23} and Poisson moduli ν_{12}, ν_{13}, ν_{23}, ν_{21}, ν_{31}, ν_{32} that characterize the layer material.

2.2.3 FE Approximation of the generalised displacement

In the case of 2D models, the discretization on the midsurface of the plate is made by means of the finite element method. The generalized displacements are in this way described as functions of the unknown nodal vector, $\mathbf{q}_{\tau i}$, and the 2D shape functions, $N_i(x, y)$:

$$\mathbf{u}_\tau^k(x, y) = N_i(x, y)\mathbf{q}_{\tau i}^k, \qquad i = 1, 2, ..., n_{elem} \tag{9}$$

where n_{elem} is the number of nodes per element and the unknown nodal vector is defined as

$$\mathbf{q}_{\tau i}^k = \left\{ \begin{array}{ccc} q_{u_{x\tau i}}^k & q_{u_{y\tau i}}^k & q_{u_{z\tau i}}^k \end{array} \right\}^T \tag{10}$$

Different sets of polynomials can be used to define FEM elements. Lagrange interpolating polynomials have been chosen in this work to generate two-dimensional elements. For the sake of brevity, their expression is not provided, but it can be found in the book by Carrera et. al,[31] in which four-node (Q4), nine-node (Q9) and sixteen-node (Q16) plate elements are described.
By combining the FEM approximation with the kinematic assumptions of the Carrera Unified Formulation, the 3D displacement field can be written as:

$$\mathbf{u}^k = F_\tau N_i \mathbf{q}_{\tau i}^k \tag{11}$$

2.2.4 Governing equations

The governing equations are obtained via the principle of virtual displacements. This variational statement sets as a necessary condition for the equilibrium of a structure that

$$\delta L_{\text{int}} + \delta L_{\text{ine}} = \delta L_{\text{e}} \tag{12}$$

The internal work is equivalent to the elastic strain energy

$$\delta L_{int}^k = \int_{V^k} \delta \boldsymbol{\varepsilon}^{kT} \boldsymbol{\sigma}^k \, dV_k \tag{13}$$

where V^k stands for the volume of the layer domain. By adopting the geometrical relation (Eq. (5)), the constitutive law (Eq. (7)), the CUF kinematic field and the FEM discretization (Eq. (11)), the internal work can be rewritten as:

$$\delta L_{\text{int}}^k = \delta \mathbf{q}_{\tau i}^{kT} \mathbf{K}^{k\tau sij} \mathbf{q}_{sj}^k \tag{14}$$

where $\boldsymbol{K}^{k\tau sij}$ is the 3×3 fundamental nucleus of the stiffness matrix.

The inertial work can be written as:

$$\delta L_{ine}^{k} = \int_{V^k} \delta \mathbf{u}^{kT} \rho^k \, \ddot{\mathbf{u}}^k \, dV_k \tag{15}$$

where ρ^k is the density of the layer material. By adopting the CUF kinematic field and the FEM discretization (Eqs. (11), it becomes:

$$\delta L_{\text{ine}}^{k} = \delta \mathbf{q}_{\tau i}^{kT} \, \mathbf{M}^{k\tau sij} \ddot{\mathbf{q}}_{sj}^{k} \tag{16}$$

where $\boldsymbol{M}^{k\tau sij}$ is the 3×3 fundamental nucleus of the mass matrix.

Finally, the external work is:

$$\delta L_{e}^{k} = \int_{V^k} \delta \mathbf{u}^{T} \mathbf{p} \, dV_k \tag{17}$$

where $\mathbf{p}$ is the vector of the external forces applied to the plate. By substituting the CUF kinematic field and the FEM discretization (Eqs. (11), one has:

$$\delta L_{\text{e}}^{k} = \delta \mathbf{q}_{\tau i}^{kT} \, \mathbf{P}^{k\tau i} \tag{18}$$

where $\boldsymbol{P}^{k\tau i}$ is the 3×1 fundamental nucleus of the nodal forces vector.

It should be noted that the formal expressions of the components of the fundamental nuclei are independent on the choice of the expanding functions F_τ, which determine the theory of structure, and shape functions N_i, which determine the numerical accuracy of the FEM approximation. This means that any plate element can be automatically formulated by appropriately expanding the fundamental nuclei according to the indexes k, τ, s, i, and j. By expanding the fundamental nuclei on the indexes τ and s the matrices of each layer are obtained. Then, the matrices of each layer are assembled at multi-layer level by imposing the continuity of the displacements at the interface between the layers (for more details, refer to[40]). Schematic of an assembled block matrix according to layer-wise approach is shown in Figure 2.

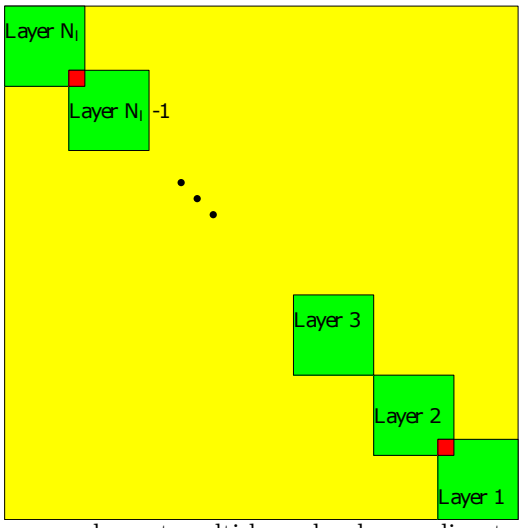

Figure 2: Assembling procedure at multi-layer level according to layer-wise approach

In this paper, the acronyms B2, B3 and B4 are used for linear, parabolic and cubic approximation through the thickness, respectively; as well as the acronyms Q4, Q9 and Q16 are used for the linear, parabolic and cubic discretization of the midsurface, respectively. According to these characteristics, the expansion order is set as a free input of the model that determines the number of unknowns to be solved.

3. RESULTS & DISCUSSIONS

In the following Figures and Tables, the CUF model results are reported and, for each value of tested Deb, the comparison of the experiments/analytical results/FE model with the data provided by the CUF models is presented.

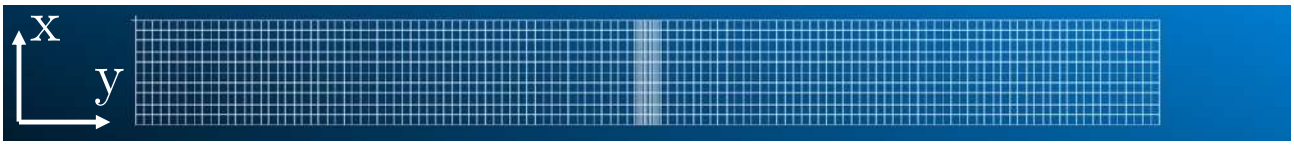

Figure 3: MSC Patran mesh

The first step for the CUF approach is the in-plane discretization of the plane geometry with Q9 elements, as shown in Figure 3. The SLJ models were meshed via MSC/PATRAN (Geometry and Elements Moduli) in order to obtain shell elements, each of which with 9 nodes. This kind of output can be obtained if the PATRAN geometrical model is exported into ABAQUS format. The modeled joint was divided into 3 areas, regarding the Lagrange expansion (by using B3 approximation for all layers) through the thickness: two of this with just one layer (aluminium plate), while the overlap zone was discretized as a 3-layers structures (aluminium-adhesive-aluminium). Particular attention was paid to the debonding area: in order to simulate the disbond between the top adherend and the adhesive, the displacement continuity among interface nodes was not imposed in that area. The spatial grid was set in order to ensure proper developing of exciting in-plane toneburst and several Lamb waves interactions (in terms of maximum wavelength); furthermore, the time step was evaluate to ensure the convergence condition by Courant-Friedrichs-Lewy (for inhomogeneous media).

Table 1: Debonding attenuation results (* indicates technical literature data reported in[29]).

Deb [mm]	N_i*	f_{att} [kHz]				Error [%]	
		Experimental*	Analytical*	FE Model*	**CUF Model**	An. vs FEM	**An. vs CUF**
5	5	230	229	240	**217**	4.8	**-5.2**
7.5		155	153	165	**149**	7.8	**-2.6**
10		116	114	115	**108**	0.9	**-5.3**
12.5		95	92	92	**104**	0.0	**13.0**
15	3	87	79	80	**73**	1.3	**-7.6**

In Table 1 and 2 the results obtained through the CUF approach are reported. For each Deb value, the excitation frequency f_{att} is reported at which a destructive experimental/analytical/numerical interference was found. These already known frequencies were compared with the one predicted by the CUF model through the presented approach. Also in this case an excellent agreement with each other was achieved, in view of the fact that CUF results were carried out by solving a much narrower Degrees of Freedom (CUF DoFs = 55629 vs Ansys DoFs = 179808). The little f_{att} difference (Deb = 12.5 mm case, grey cells in Table 1) is caused by constant grid mesh and time step. Despite each damage needs a certain spatial and time discretization, for the sake of simplicity, fixed steps were implemented for all five CUF simulations.

In Table 2 the spectrograms evaluated by application of a Short Fourier Transform to the numerical signal are shown: per each case, the destructive interference (related to relative Deb value) is clearly identified. Comparing 2^{nd} and 3^{rd} columns of Table 2, it can be seen that the observation time window reported on the y-axis of each spectrogram (3^{rd} column), represents the output signal time evolution (2^{nd} column). The "holes" spectrogram and relative PSD "cusps", can be associated to the output signal attenuations: per each row, at the "hole time", the u_y plot shows a deformed toneburst-shape due to the destructive interference between the direct signal and the reflected wave in the Deb area.

In practice, a SHM specialist should generate the toneburst signal and monitor the real-time acquisition of the propagating waveforms: the exciting frequency should be changed as long as the output signal does not contain

Table 2: CUF results.

Deb [mm]	Output Signal	Spectrogram
5	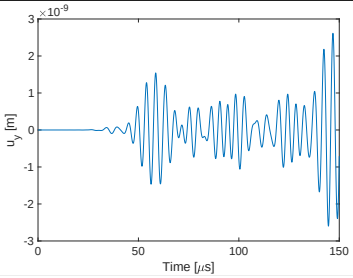	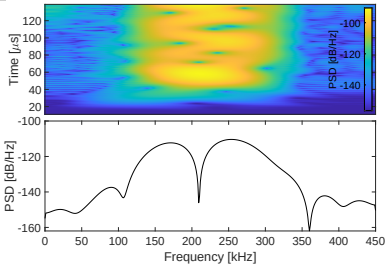
7.5	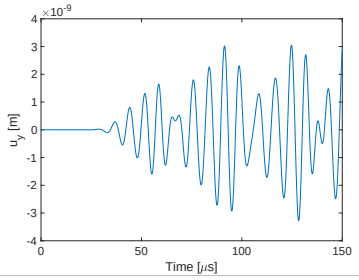	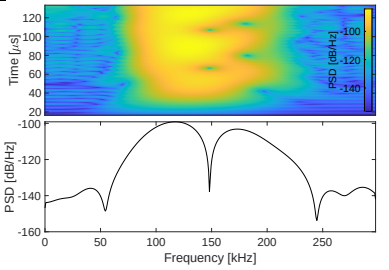
10	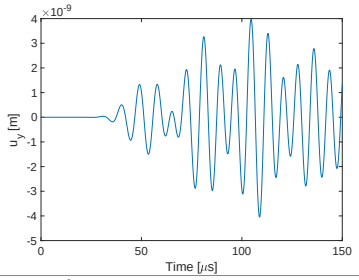	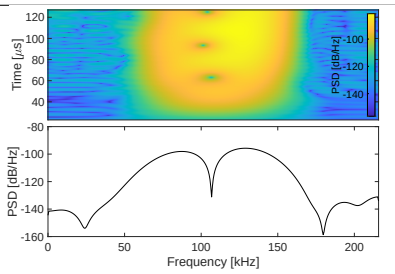
12.5	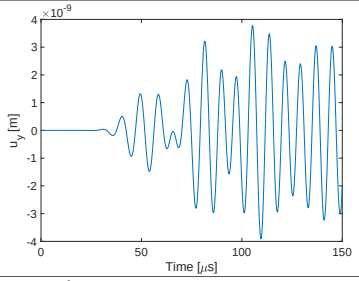	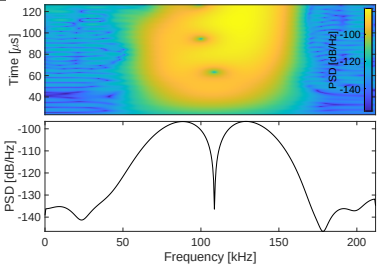
15	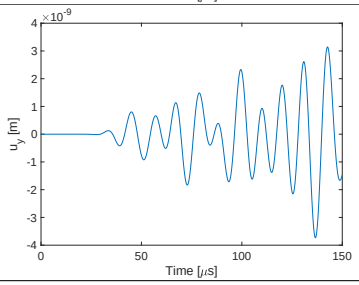	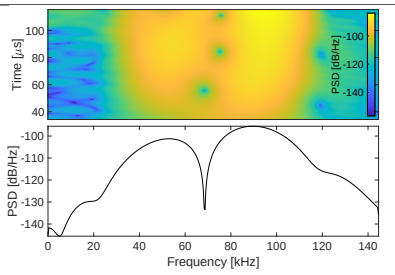

shape changes, suggesting the presence of damage in the overlap zone, in terms of waveform and frequency spectrum (as presented in 2^{nd} and 3^{rd} columns of Table 2). In the authors' opinion, the simplicity and low cost of the CUF model make it particularly interesting for SHM applications, since it can easily evaluate the certain frequency promoting destructive wave interference in a damaged SLJ and suggests (and definitely reduces) the frequency range at which a SHM specialist has to work in order to correctly identify the damage length.

4. CONCLUSIONS

In the present work the CUF model for Lamb waves interferences in SLJ is proposed as novel SHM tool. From the numerical point of view, the kinematics of the model was simulated by using Legendre Expansions polynomials. In this manner, Lamb waves and their interactions were studied via dimensionally reduced models (in comparison with standard FE models). From the experimental point of view, the SLJ samples were made of two thin aluminum plates bonded by an biadhesive layer. An artificial defect was introduced in the overlap zone between the adhesive layer and the upper plate.

The already known method showed that for each debonding value there is one excitation frequency for which a destructive interference occurs, univocally related to the defect. The CUF results show an excellent agreement with the experimental/analytical/FE data. This good correlation demonstrated the validity of the proposed CUF model for the SHM of SLJs.

Future work can be addressed to apply the same CUF approach for the delaminations detection in multilayered composite SLJ, where the CUF turns out to be particularly convenient in terms of computational efficiency.

REFERENCES

[1] Lowe, M., "Matrix techniques for modeling ultrasonic waves in multilayered media," *IEEE Transactions on Ultrasonics, Ferroelectrics, and Frequency Control* **42**(4), 525–542 (1995).

[2] Obenchain, M. B. and Cesnik, C. E. S., "Producing accurate wave propagation time histories using the global matrix method," *Smart Materials and Structures* **22**, 125024 (nov 2013).

[3] Datta, S. K., Shah, A. H., Bratton, R., and Chakraborty, T., "Wave propagation in laminated composite plates," *The Journal of the Acoustical Society of America* **83**(6), 2020–2026 (1988).

[4] Gavrić, L., "Computation of propagative waves in free rail using a finite element technique," *Journal of Sound and Vibration* **185**(3), 531–543 (1995).

[5] Bartoli, I., Marzani, A., Di Scalea, F. L., and Viola, E., "Modeling wave propagation in damped waveguides of arbitrary cross-section," *Journal of sound and vibration* **295**(3-5), 685–707 (2006).

[6] Delsanto, P., Whitcombe, T., Chaskelis, H., and Mignogna, R., "Connection machine simulation of ultrasonic wave propagation in materials. i: the one-dimensional case," *Wave motion* **16**(1), 65–80 (1992).

[7] Lee, B. and Staszewski, W., "Modelling of lamb waves for damage detection in metallic structures: Part i. wave propagation," *Smart materials and structures* **12**(5), 804 (2003).

[8] Yim, H. and Choi, Y., "Simulation of ultrasonic waves in various types of elastic media using the mass spring lattice model," *Materials evaluation* **58**(7), 889–896 (2000).

[9] Heinze, C., Duczek, S., and Sinapius, M., "A minimal model for fast approximation of lamb wave propagation in complex aircraft parts," in [*Lamb-Wave Based Structural Health Monitoring in Polymer Composites*], 241–261, Springer (2018).

[10] Ke, W., Castaings, M., and Bacon, C., "3d finite element simulations of an air-coupled ultrasonic ndt system," *Ndt & E International* **42**(6), 524–533 (2009).

[11] Carrino, S., Nicassio, F., and Scarselli, G., "Subharmonics and beating: a new approach to local defect resonance for bonded single lap joints," *Journal of Sound and Vibration* **456**, 289–305 (2019).

[12] Nicassio, F., Carrino, S., and Scarselli, G., "Non-linear lamb waves for locating defects in single-lap joints," *Frontiers in Built Environment* **6**, 45 (2020).

[13] Ng, C.-T. and Veidt, M., "Scattering of the fundamental anti-symmetric lamb wave at delaminations in composite laminates," *The Journal of the Acoustical Society of America* **129**(3), 1288–1296 (2011).

[14] Komatitsch, D. and Tromp, J., "Spectral-element simulations of global seismic wave propagation—i. validation," *Geophysical Journal International* **149**(2), 390–412 (2002).

[15] Kudela, P., Krawczuk, M., and Ostachowicz, W., "Wave propagation modelling in 1d structures using spectral finite elements," *Journal of sound and vibration* **300**(1-2), 88–100 (2007).

[16] Dedè, L., Jäggli, C., and Quarteroni, A., "Isogeometric numerical dispersion analysis for two-dimensional elastic wave propagation," *Computer Methods in Applied Mechanics and Engineering* **284**, 320–348 (2015).

[17] Willberg, C., *Development of a new isogeometric finite element and its application for Lamb wave based structural health monitoring*, PhD thesis, Magdeburg, Universität, Diss., 2012 (2013).

[18] Duczek, S., Joulaian, M., Düster, A., and Gabbert, U., "Numerical analysis of lamb waves using the finite and spectral cell methods," *International Journal for Numerical Methods in Engineering* **99**(1), 26–53 (2014).

[19] Ham, S. and Bathe, K.-J., "A finite element method enriched for wave propagation problems," *Computers & structures* **94**, 1–12 (2012).

[20] Willberg, C., Duczek, S., Perez, J. V., Schmicker, D., and Gabbert, U., "Comparison of different higher order finite element schemes for the simulation of lamb waves," *Computer methods in applied mechanics and engineering* **241**, 246–261 (2012).

[21] Hu, N., Liu, Y., Li, Y., Peng, X., and Yan, B., "Optimal excitation frequency of lamb waves for delamination detection in cfrp laminates," *Journal of composite materials* **44**(13), 1643–1663 (2010).

[22] Schulte, R. T. and Fritzen, C.-P., "Simulation of wave propagation in damped composite structures with piezoelectric coupling," *Journal of Theoretical and Applied Mechanics* **49**(3), 879–903 (2011).

[23] Schulte, R., Fritzen, C., and Moll, J., "Spectral element modelling of wave propagation in isotropic and anisotropic shell-structures including different types of damage," in [*IOP Conference Series: Materials Science and Engineering*], **10**(1), 012065, IOP Publishing (2010).

[24] de Miguel, A., Pagani, A., and Carrera, E., "Higher-order structural theories for transient analysis of multi-mode lamb waves with applications to damage detection," *Journal of Sound and Vibration* **457**, 139–155 (2019).

[25] Carrera, E., Cinefra, M., Petrolo, M., and Zappino, E., [*Finite element analysis of structures through unified formulation*], John Wiley & Sons (2014).

[26] Cinefra, M., "Non-conventional 1d and 2d finite elements based on cuf for the analysis of non-orthogonal geometries," *European Journal of Mechanics-A/Solids* **88**, 104273 (2021).

[27] Kumar, S. K., Cinefra, M., Carrera, E., Ganguli, R., and Harursampath, D., "Finite element analysis of free vibration of the delaminated composite plate with variable kinematic multilayered plate elements," *Composites Part B: Engineering* **66**, 453–465 (2014).

[28] Kumar, S. K., Harursampath, D., Carrera, E., Cinefra, M., and Valvano, S., "Modal analysis of delaminated plates and shells using carrera unified formulation–mitc9 shell element," *Mechanics of Advanced Materials and Structures* **25**(8), 681–697 (2018).

[29] Nicassio, F., Carrino, S., and Scarselli, G., "Elastic waves interference for the analysis of disbonds in single lap joints," *Mechanical Systems and Signal Processing* **128**, 340–351 (2019).

[30] Washizu, K., [*Variational Methods in Elasticity and Plasticity*], Elsevier Science & Technology (1974).

[31] E. Carrera, G. Giunta, M. P., [*Beam structures: classical and advanced theories*], John Wiley and Sons (2011).

[32] Carrera, E., Cinefra, M., Petrolo, M., and Zappino, E., [*Finite Element Analysis of Structures through Unified Formulation*], John Wiley & Sons (2014).

[33] Carrera, E., "Theories and finite elements for multilayered plates and shells: a unified compact formulation with numerical assessment and benchmarking," *Archives of Computational Methods in Engineering* **10**(3), 216–296 (2003).

[34] Carrera, E., Pagani, A., and Valavano, S., "Multilayered plate elements accounting for refined theories and node-dependent kinematics," *Composites Part B: Engineering* **114**, 189–210 (2017).

[35] Li, G., Carrera, E., Cinefra, M., de Miguel, A., Pagani, A., and Zappino, E., "An adaptable refinement approach for shell finite element models based on node-dependent kinematics," *Composites Part B: Engineering* **210**, 1–19 (2019).

[36] Cinefra, M., Valvano, S., and Carrera, E., "A layer-wise MITC9 finite element for the free-vibration analysis of plates with piezo-patches," *International Journal of Smart and Nano Materials* **6**(2), 85–104 (2015).

[37] Pagani, A., Valvano, S., and Carrera, E., "Analysis of laminated composites and sandwich structures by variable-kinematic MITC9 plate elements," *Journal of Sandwich Structures and Materials* (2016). In Press.

[38] Kulikov, G., Mamontov, A., Plotnikova, S., and Mamontov, S., "Exact geometry solid-shell element based on a sampling surfaces technique for 3d stress analysis of doubly-curved composite shells," *Curved and Layered Structures* **3**(1) (2016).

[39] Kulikov, G. and Plotnikova, S., "A method of solving three-dimensional problems of elasticity for laminated composite plates," *Mechanics of Composite Materials* **48**(1), 15–26 (2012).

[40] Carrera, E., "Theories and finite elements for multilayered, anisotropic, composite plates and shells," *Archives of Computational Methods in Engineering* **9**(2), 87–140 (2002).